JOURNAL OF MATERIALS SCIENCE 21 (1986) 3351–3356

A dislocation network model of recovery-controlled creep

O. AJAJA
Department of Physics, University of Ife, Ile-Ife, Nigeria

A new model of recovery-controlled creep deformation, based on the jerky glide motion of dislocations between obstacles, is proposed. A three-dimensional distribution of dislocation links is visualized such that only links which attain a certain threshold size, λ_a, through recovery can glide rapidly until they are again arrested at the next obstacle. The rate of mobilization of arrested dislocations is shown to be directly proportional to the annihilation rate, $\dot{\varrho}_a$. The strain rate, $\dot{\gamma}$, during transient creep is related to the annihilation rate, the obstacle spacing L and the Burgers vector $\boldsymbol{b}$ of the dislocations according to the expression

$$\dot{\gamma} = \alpha_1 \psi(t)\, \dot{\varrho}_a \boldsymbol{b} L$$

where α_1 is a geometrical constant and $\psi(t)$ is a time-dependent parameter whose value is determined by the instantaneous (free) dislocation density as well as some salient features of the dislocation distribution. At steady state, $\psi(t)$ translates into a constant which is stress and temperature independent. The average effective dislocation velocity is also shown to be directly proportional to the annihilation rate. The model is used to rationalize the familiar creep transients which are usually observed when the stress is altered abruptly during recovery creep.

1. Introduction

Dislocation creep is often classified as either glide-controlled or recovery-controlled, depending on which of the two simultaneous processes of glide and recovery is believed to be the slower. Most theories of creep are usually regarded as being successful once they predict the "correct" stress exponent for the steady-state creep rate. The characterization of transient creep has been generally less successful apparently because this creep stage does not easily lend itself to certain simplifying assumptions which are readily applicable to steady state.

In materials undergoing recovery creep, the normal primary creep stage is often accompanied by the development of subgrains whose boundaries become well defined as steady state is approached. The density of dislocations inside the subgrains (hereinafter referred to as "free" dislocations) decreases, usually by a factor of two or more during transient creep [1]. Attempts have been made to explain the decreasing creep rate by invoking the concept of subgrain strengthening [2]. However, the results of recent experimental investigations have demonstrated quite clearly that subgrain boundaries may not be potent sources of strengthening, at least at elevated temperatures [3, 4].

No less paradoxical is the material weakening associated with the inverse transient creep of several alloys in spite of increasing dislocation density [5, 6]. Creep in such alloys is believed to be glide-controlled. The problem then is essentially that of explaining the material strengthening accompanied by decreasing dislocation density on the one hand, and the weakening associated with increasing dislocation density on the other. Both of these observations are clearly in conflict with classical work-hardening models which predict increased strength as the dislocation density increases.

It is this author's firm conviction that these apparent paradoxes arise largely because not all the parameters which influence creep strength have been considered in explaining the observed transient effects. Ajaja and Ardell [3], after noting that the process of subgrain development in a stainless steel could be accompanied by material strengthening or weakening depending on the creep conditions, concluded that their observation of the microstructure may not tell the entire story. There appears to be an important, though concealed, parameter which is not being properly counted.

In recovery-controlled creep this parameter would appear to be the rate of recovery of the deforming sample. The Bailey–Orowan model [7] is widely acclaimed for its unique characterization of the relationship between the creep rate and the rate of recovery. Past experimentation also appears to have confirmed the existence of a direct parallelism between these two quantities [8, 9]. This observation however, is yet to be harmonized with the basic Taylor–Orowan equation which relates the strain rate to the dislocation density and the dislocation glide velocity. It would be interesting to know, for example, the relationship between the dislocation velocity and the recovery rate.

In this paper, the processes of dislocation obstruction by obstacles and their subsequent release through

recovery (recovery-creep) are examined. Expressions are derived for the strain rate during transient and steady-state creep in terms of the annihilation rate and other pertinent features of the dislocation structure. The significance of the dislocation velocity in the Taylor–Orowan equation is closely examined and other familiar phenomena commonly associated with creep deformation are rationalized.

2. The model

2.1. Dislocation obstruction process during recovery-creep

At sufficiently high stresses, an instantaneous plastic strain is usually generated upon loading a creep sample. It is a general characteristic of dislocation creep, especially in pure metals, that no further (creep) strain can be generated without the aid of recovery (recovery-controlled creep) and/or thermal activation (thermally-activated creep). This implies that few dislocations are long enough to continue gliding under the applied stress, i.e. most dislocations must be held up at obstacles.

In a single-phase crystalline solid, the main obstacles to dislocation glide are typically forest dislocations. The interactions between the glissile and the forest dislocations often result in the formation of a three-dimensional network of dislocation links of various sizes joined at nodes. A dislocation link can be released only if the applied stress is large enough to "unpin" a nodal junction, or to bow out the link between two nodes via the Orowan mechanism. In the case of dislocation–dislocation interactions, the former scenario seems more probable as dislocation nodes could hardly be regarded as obstacles of infinite strength.

The shear stress τ required to release a link of length λ is given by the well known relation

$$\tau = \alpha_0 G\boldsymbol{b}/\lambda \qquad (1)$$

where G is the shear modulus of the deforming crystal, α_0 is related to the strength of the obstacle and $\boldsymbol{b}$ is Burgers vector. In general, $\alpha_0 \leqslant 1$, the upper limit ($\alpha_0 = 1$) corresponding to the case of strong obstacles which can only be bypassed by Orowan bowing. It is clear that for any given stress, not all links will possess the requisite length for the bypassing of obstacles.

At high temperature, the dislocation structure coarsens by recovery, so that on average dislocation links become longer (though fewer in number), thus allowing some arrested links to be freed from their obstacles, and sustain the deformation process. The dislocation release process can also be aided by thermal activation. This model will, however, focus on the situation in which the mobilization of links is secured mainly through recovery, i.e. when the thermally activated release process is relatively insignificant. Examples of such athermal obstacles have been discussed by Ostrom and Lagneborg [10], and we assume it is generally valid for recovery-controlled creep.

Once a link is released, we suppose it can glide rapidly until it encounters the next obstacle. The obstacle partitions the link into two segments each of which may be too short to continue gliding under the applied stress (Equation 1). Each of the new segments must thus spend some finite time (during which its length increases by recovery) waiting to bypass the obstacle. After surmounting the obstacle, the link glides freely again until it encounters the next obstacle and the process repeats itself. The kinetics of this kind of dislocation obstruction process have been treated in some detail by Gillis *et al.* [11], Lloyd *et al.* [12], Frost and Ashby [13] and Kocks *et al.* [14].

2.2. Dislocation distribution and mobilization

A schematic illustration of a typical distribution function is provided in Fig. 1 where the frequency function $\phi(\lambda, t)$ is defined such that $\phi(\lambda, t)\,\mathrm{d}\lambda$ is the number of dislocation links per unit volume having lengths between λ and $\lambda + \mathrm{d}\lambda$. For materials in which subgrains develop during deformation, the distribution function incorporates only the free dislocations; dislocations in subgrain walls are not included. To mobilize a link under an applied stress τ_a, it must attain length λ_a given by Equation 1:

$$\lambda_a = \alpha_0 G\boldsymbol{b}/\tau_a. \qquad (2)$$

It is to be expected that in any three-dimensional network of dislocation links, only some of the links will lie on crystallographic planes which are favourable for glide; these are the potentially mobile links. Other links which are unfavourably oriented will be immobile. Upon loading a creep sample to a stress level τ_a, all potentially mobile links with lengths greater than λ_a should glide rapidly until they again become immobilized by interacting with the rest of the network. Thus any links in the distribution with $\lambda > \lambda_a$ after loading must be immobile (Fig. 1). The region $0 < \lambda < \lambda_a$ consists of both immobile and potentially mobile links.

The area under the frequency curve represents the total number of links, N, per unit volume, i.e.

$$N = \int_0^\infty \phi(\lambda, t)\,\mathrm{d}\lambda \qquad (3)$$

while the dislocation density is given by

$$\varrho = \int_0^\infty \phi(\lambda, t)\,\lambda\,\mathrm{d}\lambda = \langle\lambda\rangle N \qquad (4)$$

where $\langle\lambda\rangle$ is the average link length (see Fig. 1). Both N and ϱ are, of course, time dependent.

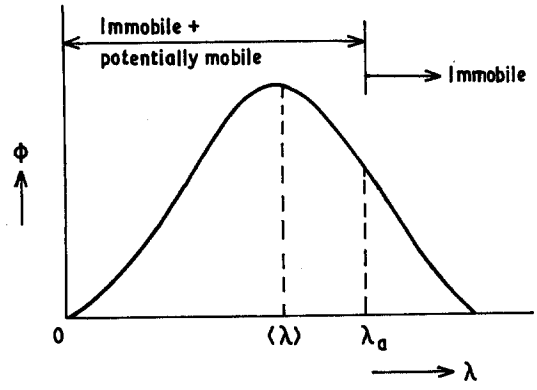

Figure 1 Schematic representation of the distribution function $\phi(\lambda, t)$ illustrating the average link length $\langle\lambda\rangle$ and the threshold link size λ_a.

2.3. Strain rate

In recovery-controlled creep, further deformation is possible after loading only if some potentially mobile links grow by recovery such that they attain lengths greater than λ_a. Suppose that creep occurs by alternate coarsening (recovery) and glide. If we picture a situation in which the distribution is held stationary while recovery occurs for time δt, some links are pumped into the region $\lambda > \lambda_a$. Without allowing further recovery, the newly generated mobile links are now allowed to glide (rapidly) and generate strain $\delta\gamma$ which is given by

$$\delta\gamma = \alpha_1 \boldsymbol{b}\delta A/V \tag{5}$$

where δA is the area swept out by gliding dislocations in a crystal of volume V, $\boldsymbol{b}$ is the Burgers vector of the dislocations and α_1 is a geometrical constant.

For the spurt-like motion of dislocations, we can write Equation 5 as

$$\delta\gamma = \alpha_1 \boldsymbol{b} A \delta N_m \tag{6}$$

where δN_m is the number of mobilized links per unit volume, each of which has swept out area A. We can further re-write Equation 6 as

$$\delta\gamma = \alpha_1 \boldsymbol{b}\left(\frac{A}{\lambda_a}\right)\cdot \lambda_a \delta N_m,$$

or

$$\delta\gamma = \alpha_1 \boldsymbol{b} L \delta\varrho_m, \tag{7}$$

where $\delta\varrho_m$ ($\equiv \lambda_a \delta N_m$) is the density of mobilized dislocations. The parameter L ($\equiv A/\lambda_a$) is closely related to the inter-obstacle spacing or the average distance through which a mobilized link glides before the next arrest. It should be recalled that λ_a is the link length upon mobilization. In the limit $\delta t \to 0$, Equation 7 gives the strain rate $\dot{\gamma} = d\gamma/dt$, or

$$\dot{\gamma} = \alpha_1 \boldsymbol{b} L \dot{\varrho}_m \tag{8}$$

where $\dot{\varrho}_m = d\varrho_m/dt$. Equation 8 has been used by past authors to characterize the strain rate during spurt-like dislocation motion [15, 16].

Within the time δt (during the recovery step) the longest links ($\lambda = \lambda_a$) would have increased their length by $\delta\lambda|_{\lambda=\lambda_a}$. The number of dislocation links thus mobilized is given by the shaded area in Fig. 2, and the density by

$$\delta\varrho_m = f_p \phi_a \lambda_a \delta\lambda|_{\lambda=\lambda_a} \tag{9}$$

where f_p is the fraction of links which are potentially mobile and ϕ_a is the value of the frequency function corresponding to the link length λ_a, i.e. $\phi_a = \phi(\lambda_a, t)$. A second order term involving $\delta\lambda|_{\lambda=\lambda_a}$ and $\delta\phi_a$, arising out of the variability of ϕ with t, is assumed to be negligibly small. Equation 9 becomes, in the limit $\delta t \to 0$

$$\dot{\varrho}_m = f_p \phi_a \lambda_a (d\lambda/dt)_{\lambda=\lambda_a}. \tag{10}$$

The value of λ_a is given by Equation 2 while $(d\lambda/dt)_{\lambda=\lambda_a}$ is the growth rate of links having length λ_a.

By analogy to grain growth theory, the growth rate of a link of length λ during recovery is given by [17]

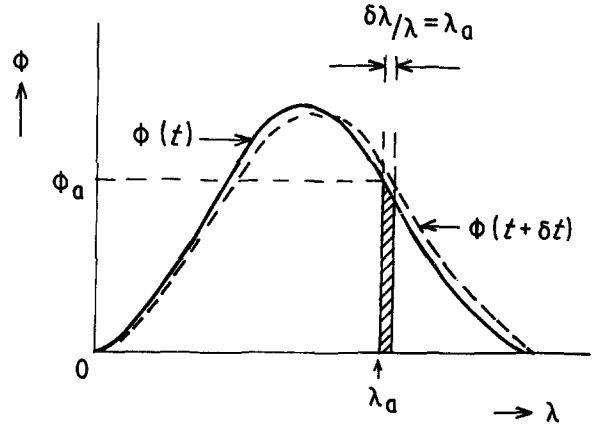

Figure 2 Schematic illustration of the number of links mobilized (shaded area) in time δt when links of threshold size would have grown by $\delta\lambda|_{\lambda=\lambda_a}$.

$$\frac{d\lambda}{dt} = k\left(\frac{1}{\lambda_c} - \frac{1}{\lambda}\right) \tag{11}$$

where k is a constant which incorporates the mobility and the line tension of the dislocations and λ_c is the critical link length. It is clear from Equation 11 that links longer than λ_c grow while shorter links shrink during recovery. The growth rate of links of length λ_a is thus

$$\left(\frac{d\lambda}{dt}\right)_{\lambda=\lambda_a} = k\left(\frac{1}{\lambda_c} - \frac{1}{\lambda_a}\right). \tag{12}$$

This quantity can be related to the overall coarsening rate of the dislocation structure, as is demonstrated below.

Ardell and Przystupa [18] recently obtained a relationship between the rate of growth of the average link, $d\langle\lambda\rangle/dt$, and the average growth rate of all the links, $\langle d\lambda/dt\rangle$, of the form

$$\left\langle\frac{d\lambda}{dt}\right\rangle = \frac{d\langle\lambda\rangle}{dt} + \frac{\langle\lambda\rangle}{N}\frac{dN}{dt}. \tag{13}$$

The volume conservation condition can be stated as [19]

$$N\langle\lambda\rangle^3 = \text{constant} \tag{14}$$

which yields, upon differentiating,

$$\frac{dN}{dt} \propto -\langle\lambda\rangle^{-4} d\langle\lambda\rangle/dt \tag{15}$$

whereupon Equation 13 becomes

$$\left\langle\frac{d\lambda}{dt}\right\rangle = -2\frac{d\langle\lambda\rangle}{dt}. \tag{16}$$

From Equation 11,

$$\left\langle\frac{d\lambda}{dt}\right\rangle = \frac{k}{\langle\lambda\rangle}\left(\frac{\langle\lambda\rangle}{\lambda_c} - \langle\lambda\rangle\langle\lambda^{-1}\rangle\right) \tag{17}$$

which, combined with Equation 16 gives

$$\frac{d\langle\lambda\rangle}{dt} = \frac{k}{2\langle\lambda\rangle}\left(\langle\lambda\rangle\langle\lambda^{-1}\rangle - \frac{\langle\lambda\rangle}{\lambda_c}\right) \tag{18}$$

Setting $\langle\lambda^{-1}\rangle = a_1\langle\lambda\rangle^{-1}$ and $\lambda_c = a_2\langle\lambda\rangle$, Equation 18 becomes

$$\frac{d\langle\lambda\rangle}{dt} = \frac{k}{\langle\lambda\rangle}\left(\frac{a_1a_2 - 1}{2a_2}\right) \quad (19)$$

Combining Equation 19 with Equation 12 we obtain

$$\left(\frac{d\lambda}{dt}\right)_{\lambda=\lambda_a} = \psi_0(t)\frac{d\langle\lambda\rangle}{dt} \quad (20)$$

where

$$\psi_0(t) = 2\left(\frac{1 - a_2\langle\lambda\rangle/\lambda_a}{a_1a_2 - 1}\right). \quad (21)$$

It should be noted that the parameters a_1 and a_2 are not necessarily constant. Indeed their time-dependences will be determined by the manner of evolution of the distribution function $\phi(\lambda, t)$. The growth rate of links of length λ_a is related to the overall coarsening rate of the network through Equation 20. The time dependence of $\psi_0(t)$ derives from those of a_1, a_2 and $\langle\lambda\rangle$.

The density of dislocations mobilized per unit time is given by Equations 10 and 20:

$$\dot{\varrho}_m = f_p\phi_a\lambda_a\psi_0(t)\frac{d\langle\lambda\rangle}{dt} \quad (22)$$

By assuming that the network geometry remains reasonably constant during deformation, the average mesh size can be taken to be directly proportional to the average link length. The proportionality constant is expected to be close to 1, so that the average link length can be related to the dislocation density according to the expression

$$\langle\lambda\rangle = \varrho^{-1/2}. \quad (23)$$

Differentiating Equation 23 with respect to t and recognizing that $\dot{\varrho} = -\dot{\varrho}_a$ (the annihilation rate) during recovery in the absence of glide, we have

$$\frac{d\langle\lambda\rangle}{dt} = \tfrac{1}{2}\varrho^{-3/2}\dot{\varrho}_a. \quad (24)$$

Substituting for λ_a (Equation 2) and $d\langle\lambda\rangle/dt$ (Equation 24) in Equation 22 gives a relationship between the mobilization and annihilation rates:

$$\dot{\varrho}_m = \psi(t)\dot{\varrho}_a \quad (25)$$

where

$$\psi(t) = \frac{\alpha_0 G\boldsymbol{b}f_p}{2\tau_a}\varrho^{-3/2}\phi_a\psi_0(t). \quad (26)$$

The strain rate is found by substituting Equation 25 into Equation 8:

$$\dot{\gamma} = \alpha_1\psi(t)\dot{\varrho}_a\boldsymbol{b}L. \quad (27)$$

Equation 27 is valid for both transient and steady-state creep. An explicit strain–time relationship cannot be obtained from this equation at the moment because the time dependences of $\psi(t)$ and $\dot{\varrho}_a$ are not known.

We can re-write Equation 24 as

$$\dot{\varrho}_a = 2\varrho^{3/2}\frac{d\langle\lambda\rangle}{dt},$$

which combined with Equations 19 and 23 yields

$$\dot{\varrho}_a = \frac{k\varrho^2(a_1a_2 - 1)}{a_2}. \quad (28)$$

It is clear from Equation 28 that the usual assumption that $\dot{\varrho}_a$ is directly proportional to ϱ^2 is valid only if a_1 and a_2 are constant. Obviously, this will depend on the exact form of the distribution function and how it evolves during creep. The evolution of the distribution function will also determine, to a large extent, the time-dependence of $\psi(t)$. These parameters are being studied in detail and the results of our findings will be reported in future publications.

Notwithstanding the difficulties mentioned above, the attractive feature of Equation 27 lies in its prediction of a direct correlation between the strain rate and a recovery parameter (i.e. the annihilation rate) during recovery-controlled creep. Moreover, a cursory inspection of Equations 21 and 26 reveals that the time dependence of $\psi(t)$ will, in general, be quite mild. If, for example, both a_1 and a_2 are assumed not to vary significantly with t, the time dependence of $\psi_0(t)$ will derive mainly from that of $\langle\lambda\rangle$: $\psi_0(t)$ will decrease as ϱ decreases (i.e. as $\langle\lambda\rangle$ increases) during normal primary creep. The value of ϕ_a will be expected to increase with increasing dislocation density (since the number of links having length λ_a should increase proportionally), though the exact relationship is not known. Thus in Equation 26, the quantities $\psi_0(t)$ and ϕ_a would decrease while $\varrho^{-3/2}$ increases as ϱ decreases. These counter-balancing effects are likely to result in a relatively mild variation of $\psi(t)$ during creep.

The purpose of going through the sketchy analysis in the foregoing paragraph is to demonstrate that the variation of $\dot{\gamma}$ during transient creep will be largely determined by the time dependence of the annihilation rate (Equation 27). Of course, the parameter L ($\cong\varrho^{-1/2}$) will increase slightly while f_p (Equation 26) can be reasonably assumed to stay constant during creep. The results of past experimental investigations have revealed that the rate of recovery decreases significantly during normal primary creep, in some cases by several orders of magnitude [8, 9]. If we assume a one-to-one correspondence between the rate of recovery and the annihilation rate, it becomes quite clear why the parallelism between the creep rate and the recovery rate is present in recovery-creep.

2.3.1. Steady-state creep

New dislocations are generated each time a released link glides through the free glide distance ($\sim L$) and increases its length in the process. It is reasonable to assume that the dislocation generation rate $\dot{\varrho}_g$ is directly proportional to the mobilization rate $\dot{\varrho}_m$, i.e.

$$\dot{\varrho}_g = \beta\dot{\varrho}_m \quad (29)$$

where β is a constant whose value would depend mainly on the link geometry during glide. At steady state the generation and the annihilation rates must be equal for the dislocation density to remain constant. Equation 29 combined with Equation 8 then gives

$$\dot{\gamma}_s = \alpha\dot{\varrho}_a\boldsymbol{b}L \quad (30)$$

where α ($\equiv\alpha_1/\beta$) is a constant and the subscript s stands for steady state. By comparing Equations 27 and 30, it is clear that at steady state,

$\psi(t) = \psi_s = 1/\beta$, i.e. ψ_s will be stress and temperature independent.

Equation 30 is not really new; it has been successfully applied to steady state (recovery-controlled) creep by other authors [20, 21]. The stress as well as the temperature dependence of the steady state creep rate derives from those of the annihilation rate and the obstacle spacing. Using this equation, Blum came up with a stress exponent of about four for the creep rate [20].

2.4. Stress change tests

It is possible in the light of the present approach, to make a few qualitative predictions about the nature of creep transients which usually follow stress changes. If the stress on a sample creeping at steady state is abruptly increased from τ_{a_1} to τ_{a_2} for example, the threshold link size decreases instantaneously from λ_{a_1} to λ_{a_2} (Fig. 3). The potentially mobile links with length λ such that $\lambda_{a_2} < \lambda < \lambda_{a_1}$ (shaded area in Fig. 3) are mobilized instantly, thus generating an instantaneous plastic strain, as is often observed following a stress increase [22, 23]. The newly generated dislocations, as well as the new unstable network, are prone to recovery. The subsequent creep process is essentially the same as that which obtains following the usual instantaneous loading strain in an annealed material.

Poirier [24] has demonstrated that the interpretation of creep data following a stress drop is less straightforward. Consider what happens, for example when the stress on a creeping sample is reduced from τ_{a_1} to τ_{a_3} in which case λ_{a_1} increases to λ_{a_3} (Fig. 3). Since there are no potentially mobile links longer than λ_{a_3} (each of the few links which happen to be gliding at the moment of stress interruption will almost instantly become arrested at the nearest obstacle), no plastic strain should be observed until links of length λ_{a_1} (the longest potentially mobile links) have grown to λ_{a_3} through recovery. This prescribes, in effect, that an incubation period should always follow a stress reduction. The nature of the subsequent creep will depend on the behaviour of the annihilation rate as well as the manner of evolution of the distribution function at the lower stress (Equation 27).

It should be noted that the creep behaviour after the stress drop could be complicated by several other factors among which are:

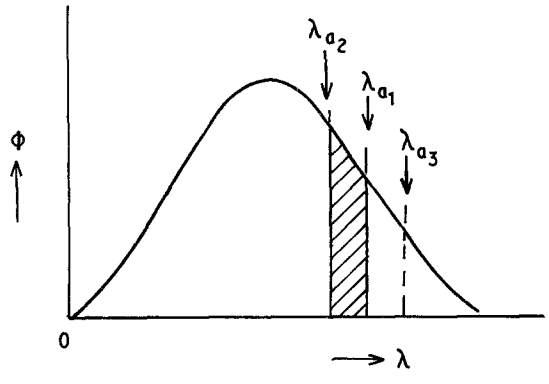

Figure 3 Schematic illustration of the threshold link size after a stress increase (λ_{a_2}), and after a stress reduction (λ_{a_3}).

1. the generation of anelastic (backward) strains due to the unbowing of bowed-out dislocation segments;

2. thermally-activated (forward) creep resulting from the thermally-activated release of some links which are otherwise too short to glide under the new stress, and

3. forward creep which might result from network coarsening [18, 25].

These may be especially significant during the period required for links of length λ_{a_1} to grow to the new length λ_{a_3} necessary for glide.

2.5. Effective dislocation velocity

In describing high temperature deformation, it has been common practice to characterize the strain rate with the familiar Taylor–Orowan equation

$$\dot{\gamma} = \alpha_1 \varrho b v \tag{31}$$

where v is the dislocation velocity. Since the value of ϱ which is often used in Equation 31 is the measured free dislocation density, it is clear that v should be some kind of average effective velocity for all the free dislocations, including those that are arrested at any given instant. This velocity is easily found by comparing Equations 27 and 31:

$$v = \frac{\psi(t)\dot{\varrho}_a}{\varrho^{3/2}} \tag{32}$$

where L has been taken to be equal to $\varrho^{-1/2}$. At steady state, this velocity becomes

$$v_s = \frac{\psi_s \dot{\varrho}_a}{\varrho_s^{3/2}}. \tag{33}$$

The implications of Equations 32 and 33 are not only physically reasonable, but are in fact expected from a correctly formulated recovery model of creep deformation. Suppose, for instance, that we have two structures of the same dislocation density which happen to be recovering at different rates (this is possible if the distributions are different; see Equation 28). Equation 33 stipulates that dislocations would, on average, move faster in the one in which recovery is more rapid. If, on the other hand, two structures recovering at the same rate have different values of ϱ, the one with the lower dislocation density would have a higher value of v.

This analysis is also consistent with the observations of Barrett *et al.* [1] and Sikka *et al.* [26] who after measuring the decrease in $\dot{\gamma}$ and ϱ during normal primary creep in various materials, concluded that v must decrease for their data to be compatible with Equation 31. It is now clear from Equation 32 that the decrease in v must be a direct consequence of a relatively large decline in the rate of recovery during this creep stage.

Phenomenological expediency has often led, in the past, to the introduction of the concept of internal stress into the strain rate equation through its influence on the effective dislocation velocity [27]. However, it is clear from Equation 32 that v is not a "glide" velocity *per se*, since its value is determined more by the rate of release of arrested dislocations than by the

details of the glide process itself. To be physically meaningful in view of the new perspective on v, the internal stress must be related principally to the process of dislocation mobilization; it is not a long range resistance to the glide motion of dislocations. This new viewpoint tends to lend support to the earlier attempt by this author at formulating a phenomenological relationship between internal stress and the rate of recovery [28].

3. Concluding remarks

The approach taken in this paper, based on the spurt-like motion of dislocation links in a three-dimensional network, has demonstrated clearly the prominent roles played by two major factors during crystal deformation. The first, and the more familiar one, is the number density of obstacles, which is important to the extent that it determines the inter-obstacle spacing within which a dislocation link can glide freely. The second, and perhaps more important factor, which ironically has often been neglected in theories of crystal deformation, is the rate of release of arrested dislocations. During the creep of pure metals the former is determined by the dislocation density and the latter by the rate of recovery.

The temptation to explain transient creep behaviour solely on the basis of the "static" dislocation structure has led to the invocation of subgrain strengthening. This, as mentioned earlier, is not justified by the results of recent experimentation, nor is it even considered necessary in the light of this model. Problems commonly encountered with the interpretation of transient creep data are easily avoided once the importance of the recovery rate is acknowledged. Its significance, which has been highlighted by the Bailey–Orowan model, is further underscored by our newly formulated equations which establish direct correlations between the strain rate and the annihilation rate. A paper which shows that the Bailey–Orowan equation in fact follows directly from these (new) equations is under preparation.

The observation that the recovery rate may not be uniquely related to the dislocation density shows why a simple correlation will not always be found between the strength of a creeping sample and the instantaneous dislocation structure observable metallographically. The magnitude of the strain rate, according to Equation 27, is essentially an indication of how fast the dislocation structure is evolving at any instant during recovery-creep, as determined by the instantaneous value of $\dot{\varrho}_a$. The shape of the creep curve (i.e. sign of $\ddot{\gamma}$), on the other hand, should be closely related to the direction of evolution, i.e. whether the dislocation structure is becoming more recovery-resistant or recovery-prone. The normal transients ($\ddot{\gamma} < 0$) characteristic of recovery-creep must thus be due, at least in part, to the concomitant rapid decline in the rate of recovery, in conformity with experimental evidence. Further understanding of the new strain rate equation, and of transient creep behaviour in particular, must await the appropriate characterization of the annihilation rate and the dislocation distribution.

Acknowledgements

Some of the basic ideas presented in this paper were originally developed jointly with Professor Alan Ardell of the Materials Science and Engineering Department, University of California, Los Angeles, USA. The author is grateful for his invaluable contributions. Partial funding provided by the US National Science Foundation under Grant Number DMR-81-11133 while the author was on leave at UCLA is gratefully acknowledged.

References

1. C. R. BARRETT, W. D. NIX and O. D. SHERBY, *Trans. ASM* **59** (1966) 3.
2. O. D. SHERBY, R. H. KLUNDT and A. K. MILLER, *Met. Trans.* **8A** (1977) 843.
3. O. AJAJA and A. J. ARDELL, *Phil. Mag.* **A39** (1979) 65.
4. J. L. ADELUS, V. GUTTMAN and V. D. SCOTT, *Mater. Sci. Eng.* **44** (1980) 195.
5. C. N. AHLQUIST and W. D. NIX, *Acta Metall.* **19** (1971) 373.
6. R. HORIUCHI and M. OTSUKA, *Trans. Jpn Inst. Metals.* **13** (1972) 284.
7. E. OROWAN, *J. West Scotland Iron Steel Inst.* **54** (1946) 45.
8. W. J. EVANS and B. WILSHIRE, *Met. Sci. J.* **4** (1970) 89.
9. T. H. ALDEN, *Metall. Trans.* **8A** (1977) 1857.
10. P. OSTROM and R. LAGNEBORG, *J. Eng. Mater. Tech. (Trans. ASME* Series H) **98** (1976) 114.
11. P. P. GILLIS, J. J. GILMAN and J. W. TAYLOR, *Phil. Mag.* **20** (1969) 279.
12. D. J. LLOYD, P. J. WORTHINGTON and J. D. EMBURY, *ibid.* **22** (1970) 1147.
13. H. J. FROST and M. F. ASHBY, *J. Appl. Phys.* **42** (1971) 5273.
14. U. F. KOCKS, A. S. ARGON and M. F. ASHBY, *Prog. Mater. Sci.* **19** (1975) 68.
15. H. MECKING and K. LUCKE, *Scripta Metall.* **4** (1970) 427.
16. R. LAGNEBORG and B. -H. FORSEN, *Acta Metall.* **21** (1973) 781.
17. A. ODEN, E. LIND and R. LAGNEBORG, in Proceedings of the Meeting on Creep Strength in Steel and High Temperature Alloys, Sheffield, 1972 (Iron and Steel Institute), p. 60.
18. A. J. ARDELL and M. A. PRZYSTUPA, *Mech. Mater.*, in press.
19. U. F. KOCKS and H. MECKING, *J. Eng. Mater. Tech. (Trans. ASME* Series H) **98** (1976) 114.
20. W. BLUM, *Phys. Status Solidi (b)* **45** (1971) 561.
21. J. HAUSSELT and W. BLUM, *Acta Metall.* **24** (1976) 1027.
22. H. OIKAWA, M. MAEDA and S. KARASHIMA, *Scripta Metall.* **6** (1972) 339.
23. V. PONTIKIS, *Acta Metall.* **25** (1977) 847.
24. J. P. POIRIER, *ibid.* **25** (1977) 913.
25. T. HASEGAWA, T. YAKOV and U. F. KOCKS, *ibid.* **30** (1982) 235.
26. V. K. SIKKA, H. NAHM and J. MOTEFF, *Mater. Sci. Eng.* **20** (1975) 55.
27. R. GASCA-NERI, C. N. AHLQUIST and W. D. NIX, *Acta Metall.* **18** (1970) 655.
28. O. AJAJA, *Scripta Metall.* **15** (1981) 975.

Received 10 May 1985
and accepted 11 April 1986